

SANDIA REPORT

SAND96-2061 • UC-704

Unlimited Release

Printed October 1996

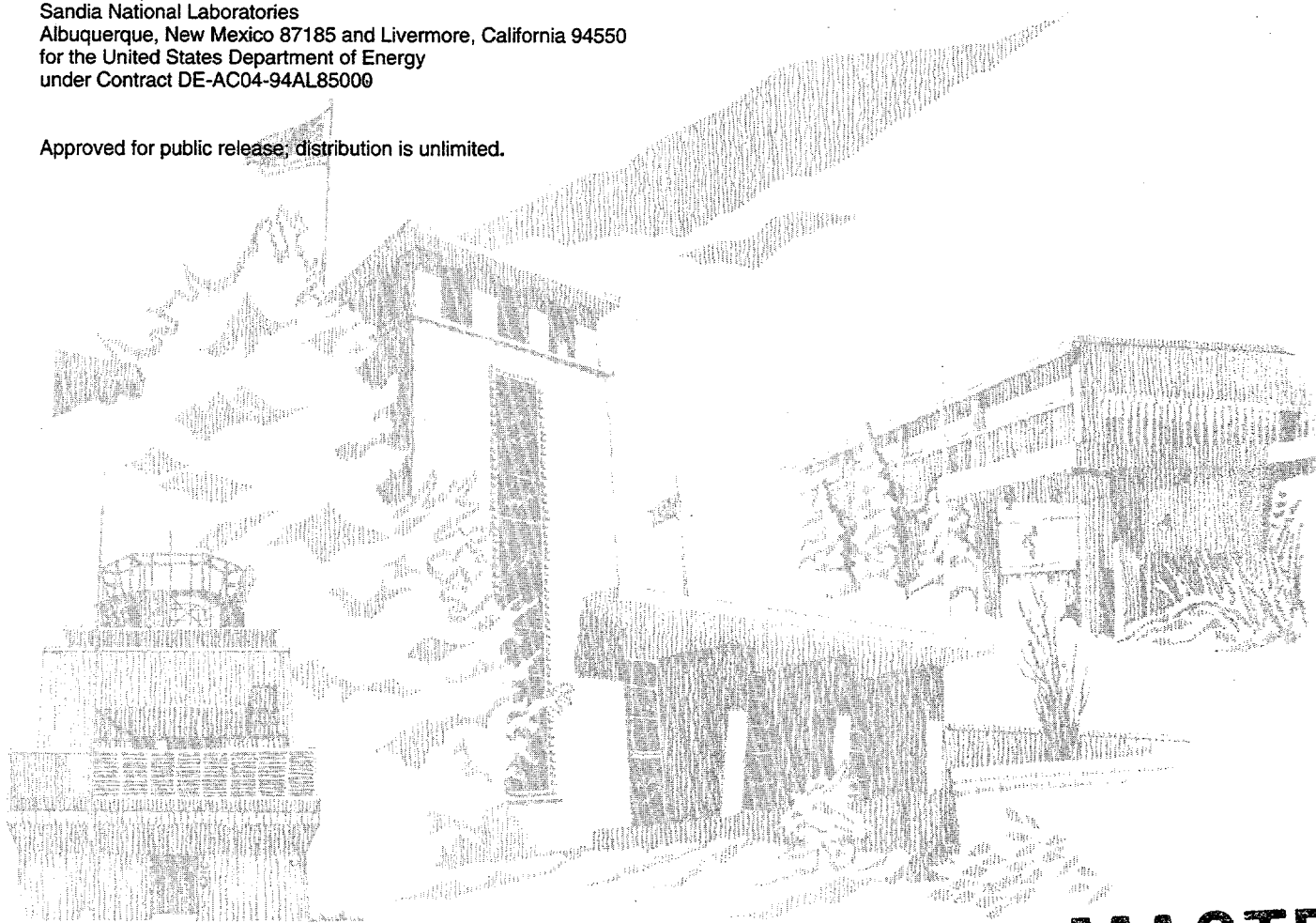
RECEIVED
FEB 12 1996
OSTI

Evaluation of the Porous Silicon Capacitor as a Moisture Sensor for Vacuum Applications

K. R. Zavadil, G. T. Cordes, M. J. Kelly, T. R. Guilinger

Prepared by
Sandia National Laboratories
Albuquerque, New Mexico 87185 and Livermore, California 94550
for the United States Department of Energy
under Contract DE-AC04-94AL85000

Approved for public release; distribution is unlimited.



Issued by Sandia National Laboratories, operated for the United States Department of Energy by Sandia Corporation.

NOTICE: This report was prepared as an account of work sponsored by an agency of the United States Government. Neither the United States Government nor any agency thereof, nor any of their employees, nor any of their contractors, subcontractors, or their employees, makes any warranty, express or implied, or assumes any legal liability or responsibility for the accuracy, completeness, or usefulness of any information, apparatus, product, or process disclosed, or represents that its use would not infringe privately owned rights. Reference herein to any specific commercial product, process, or service by trade name, trademark, manufacturer, or otherwise, does not necessarily constitute or imply its endorsement, recommendation, or favoring by the United States Government, any agency thereof or any of their contractors or subcontractors. The views and opinions expressed herein do not necessarily state or reflect those of the United States Government, any agency thereof or any of their contractors.

Printed in the United States of America. This report has been reproduced directly from the best available copy.

Available to DOE and DOE contractors from
Office of Scientific and Technical Information
PO Box 62
Oak Ridge, TN 37831

Prices available from (615) 576-8401, FTS 626-8401

Available to the public from
National Technical Information Service
US Department of Commerce
5285 Port Royal Rd
Springfield, VA 22161

NTIS price codes
Printed copy: A03
Microfiche copy: A01

DISCLAIMER

This report was prepared as an account of work sponsored by an agency of the United States Government. Neither the United States Government nor any agency thereof, nor any of their employees, makes any warranty, express or implied, or assumes any legal liability or responsibility for the accuracy, completeness, or usefulness of any information, apparatus, product, or process disclosed, or represents that its use would not infringe privately owned rights. Reference herein to any specific commercial product, process, or service by trade name, trademark, manufacturer, or otherwise does not necessarily constitute or imply its endorsement, recommendation, or favoring by the United States Government or any agency thereof. The views and opinions of authors expressed herein do not necessarily state or reflect those of the United States Government or any agency thereof.

DISCLAIMER

Portions of this document may be illegible in electronic image products. Images are produced from the best available original document.

Evaluation of the Porous Silicon Capacitor as a Moisture Sensor for Vacuum Applications

K.R. Zavadil, G.T. Cordes, M.J. Kelly
and T.R. Guilinger
Surface & Sensor-Controlled Processes Department
Sandia National Laboratories
Albuquerque, NM 87185-0333

Abstract

A growing demand exists for inexpensive and reliable sensors for moisture detection in reduced pressure processing environments. Sandia's Porous Silicon Capacitor (PSC) sensor appears to be an ideal candidate for this application. This sensor is a solid state device that detects moisture through changes in dielectric constant with water adsorption. Standard microelectronic fabrication techniques are used in its production affording low cost production and ready integration into complex sensor and electronic arrays. This sensor has previously been investigated for moisture detection in fluid streams, however, little effort has been placed on its behavior in a vacuum environment. Sandia's Sensors in Vacuum (SIV) test facility has been employed to evaluate the performance characteristics of this sensor in vacuum. In addition, a vacuum-based study allows for a more controlled environment in which the intrinsic lower limit for moisture detection and response times to moisture changes can be easily determined quantitatively. This report describes the performance characteristics of a series of sensors from a single production lot. Calibration of these sensors to moisture levels from part per billion to part per hundred concentrations has been performed. The concentration-dependent sensitivity of these sensors is documented. The response time and drift characteristics of these sensors are also discussed. The investigation of a preliminary method for increasing the recovery time of the sensor after moisture exposure is presented. The role of hydrocarbon contamination, a potential problem in some vacuum schemes, is also evaluated. Specific recommendations are made on how to implement this sensor for vacuum applications.

MASTER

I. Introduction

Sandia's porous silicon capacitor (PSC) sensor has the potential of being developed into a cost effective device for moisture detection in vacuum applications. The PSC is a solid state device that is produced using a series of conventional vacuum and wet chemical processes. These devices can be produced in quantities of 4000 to 5000 per 8 inch wafer. The average device size is on the order of 2x2 mm and the header to which the die is bonded has a nominal diameter of 8 mm. In addition to their compact nature, these devices have been shown to be robust, stable moisture monitors in various environments [1-4]. An approximate cost estimate for production is several dollars per sensor. Measurement electronics could be greatly simplified to a simple resonator circuit with an estimated production cost of ~\$50 per circuit. Vacuum integration requires mounting on commercially available electrical feedthroughs. These devices are well suited for contaminant-free processing environments because of their compatibility with silicon processing environments.

The moisture sensitivity of the PSC results from water adsorption within a high surface area porous silicon (PS) layer. PS is formed from single crystal silicon wafers by electrochemical anodization in a hydrofluoric acid electrolyte. The remainder of the steps in fabricating a PSC sensor are standard microelectronic processes. The moisture sensor shown in Figure 1 functions as a variable capacitance device. Water vapor that contacts the sensor diffuses through the openings in the aluminum grid top electrode. The water is transported through the porous microstructure where it adsorbs onto the pore walls and/or condenses in the pores via capillary condensation. The amount of water in the porous silicon structure directly affects the dielectric constant. Changes in dielectric constant are measured in the form of a capacitance using the

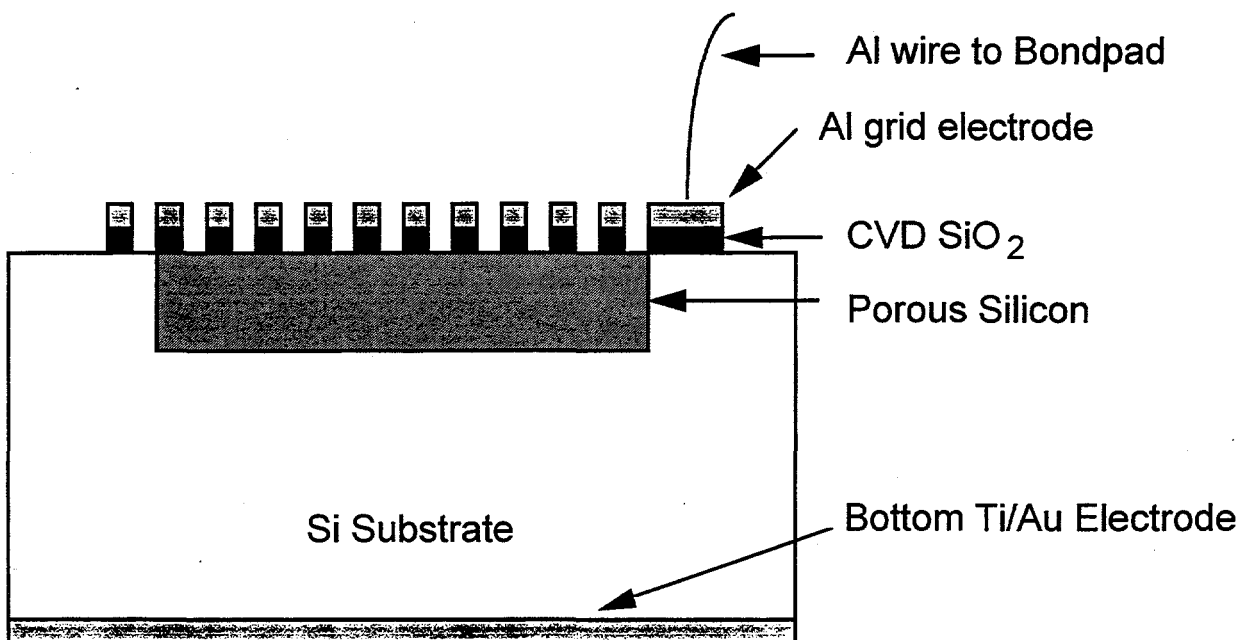


Figure 1: Cross-section View of an Aluminum Grid PSC Moisture Sensor electrodes of the sensor.

In this report, the properties of this sensor in a reduced pressure environment are described. Representative members of a single production lot were calibrated. Estimates of lower limit of moisture detection as well as the response times for pressure increases and decreases were determined. Atmospheric venting studies were conducted to simulate behavior under load lock conditions. The effects of extended vacuum containment on moisture sensitivity were investigated. Error estimates are made for baseline capacitance drift in these sensors. The impact of operational aging and contaminants on the sensors' response is also discussed.

II. Experimental Methods

The experiments described in this report were conducted in Sandia's Sensors in Vacuum (SIV) test system. The SIV system was designed for precise control and measurement of moisture levels in a reduced pressure environment. The system is an all metal, ultrahigh vacuum chamber that is pumped with a 400 L/sec Alcatel (ATP 5400 CP) turbomolecular pump. The chamber is separated from the pump with a VAT (Series 20) UHV butterfly valve with a bored gate. Stainless steel foils with set diameter bore holes, ranging from 10 to 2.5 mm diameter, can be mounted on the gate face to provide a conductance limited orifice. Pressures as high as 1 torr H₂O can be produced without significantly compromising the compression ratio of the turbo pump. This upper limit places controlled exposure slightly below typical atmospheric levels for moisture. H₂O is introduced into this chamber using a Granville-Phillips (Series 216) precision leak valve that is stepper motor controlled. Pressure feedback from one of several transducers provides for precise input flow and pressure regulation. A sealed ampoule of pyrolytically distilled H₂O serves as a vapor source. Dissolved gases were removed from the H₂O using multiple freeze-pump-thaw cycles. Water vapor purity was demonstrated using a residual gas analyzer.

A system of transfer standards are used for quantitative pressure measurement in the SIV chamber. A Granville-Phillips Sabil-1™ ion gauge (Series 360) is used for measurement from base pressure (1×10^{-9} torr) up to 1×10^{-4} torr. A MKS SRG 2 spinning rotor gauge (SRG) is used for pressures of 5×10^{-7} to 0.1 torr. Viscosity corrections for H₂O are made for measurements above 1×10^{-2} torr. Both of these gauges routinely undergo calibration at Sandia using NIST-traceable methods. The SRG has been used to establish zero-corrected baselines for a pair of MKS thermostated capacitance diaphragm gauges (Model 120AA) that allow for pressure measurement from 1×10^{-3} to 1 torr. Any of these gauges can be used to control the precision leak valve using a control and data acquisition program designed to operate on an IBM compatible personal computer. We have demonstrated control of H₂O pressure from 1×10^{-9} to 1 torr.

The PSC sensors used in this study were generated from a single production lot. They consist of a capacitance sensor, an integrated heater and a temperature sensitive diode mounted on an open TO-39 header. The top Al grid electrode for the capacitor was wire-bonded to allow its use as a heater element. The leads on the TO-39 header were spot welded to the leads of a KF-40 electrical feedthrough. The capacitor electrodes were mounted to two BNC pins while the heater lead and one lead of the diode were welded to two power leads. The back of the die served as a capacitor electrode and as a second diode connection. Capacitance measurements were made with a Keithley Model 3330 LCZ meter at a frequency of 10 kHz and an amplitude of 1V. Current to heat the sensor was supplied by an HP 6024A power supply. Sensor temperature measurements were made with an HP 6625A voltmeter using a 100 μ A bias current applied to the diode.

The PSC sensors were fabricated by first depositing a 1200 nm silicon nitride mask on the surface of a (100), p-type, 0.14-0.3 Ω -cm silicon wafer. The silicon nitride was patterned and etched by a combination of photolithography and etching techniques to create numerous 2 mm x 2 mm openings in the mask. These exposed silicon regions were then made porous by electrochemical anodization in 5 wt.% hydrofluoric acid at 5.9 mA/cm² for 252 seconds. This produced a 1 μ m thick PS layer with a porosity of 80%. A PS layer fabricated in this fashion is characterized by a highly interconnected, isotropic porous structure (i.e., a “sponge-like” morphology) with pores having cross-section diameters ranging from 2-10 nm. Next, the chemical reagent tetraethoxyorthosilicate (TEOS) was used in the deposition of a 100 nm layer of plasma-enhanced chemically vapor deposited (PECVD) silicon dioxide (designated as CVD SiO₂ in Figure 1) onto the wafers. This was followed by deposition of 1 μ m of aluminum onto the CVD oxide. Finally, the aluminum and CVD oxide were patterned and etched into a grid pattern by a combination of photolithography and etching steps. In this sensor, 2 μ m wide grid lines are separated by 2 μ m wide openings. Blanket layers of titanium/gold were then deposited on the backs of the wafers to produce the device shown in Figure 1.

III. Results

III.1 General Response to H₂O Vapor

The PSC sensors have a five decade dynamic range of moisture detection. Figure 2 shows the

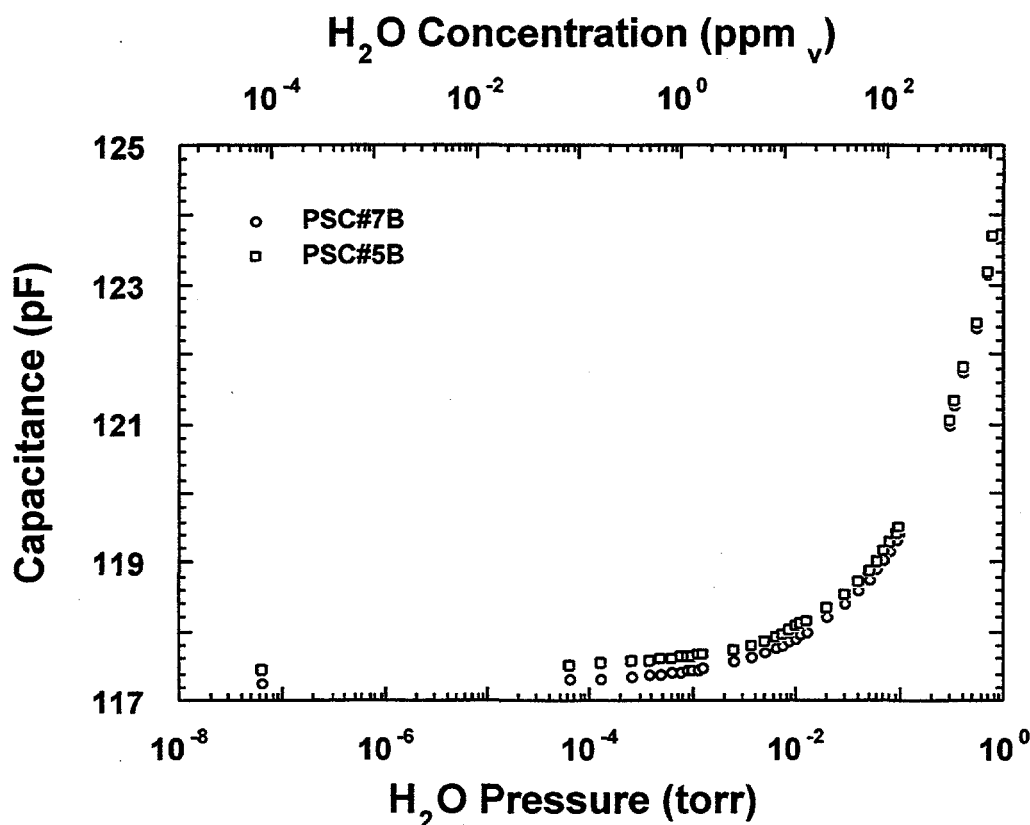


Figure 2: Variation in PSC Response with H₂O Pressure

response of two sensors to increasing H₂O pressure. The calibration was conducted using pressure steps that ranged from 60 minutes at the lowest pressures to less than 5 minutes at the highest pressures. The goal in using a variable time exposure was to allow for adequate equilibration of the sensor. Pressure was regulated to within $\pm 1\%$ over this range. The lowest pressure data point shown in this plot is the dry or baseline capacitance (C_b) of these sensors. These sensors have been subjected to a 60 hour period of vacuum containment with a H₂O partial pressure less than 2×10^{-8} torr to ensure an initial, dry state. The data show that differences greater than several tenths of a picofarad can exist between the C_b values for sensors in a production lot. The data also show that the first response of these sensors to H₂O vapor occurs at pressures as low as 5×10^{-5} torr. Increased pressure produces an increase in capacitance for both sensors. A larger absolute change is observed with each additional order of magnitude pressure increase. This observation is consistent with an increase in adsorbed H₂O content with increased pressure yielding larger changes in dielectric constant for the porous Si layer. The magnitude of capacitance change with pressure appears similar for these sensors indicative of similar sensitivities despite differences in C_b values.

III.2 PSC Sensitivity and Lower Limit of Moisture Detection

Significant variation in the sensitivity to moisture exists within a production lot of PSC sensors. Figure 3 shows the relative responses of seven different sensors to variations in H₂O pressure over a range of 1×10^{-4} to 0.1 torr. The absolute capacitance values have been converted to difference values by subtracting a sensor's C_b value. All sensors show a similar non-linear

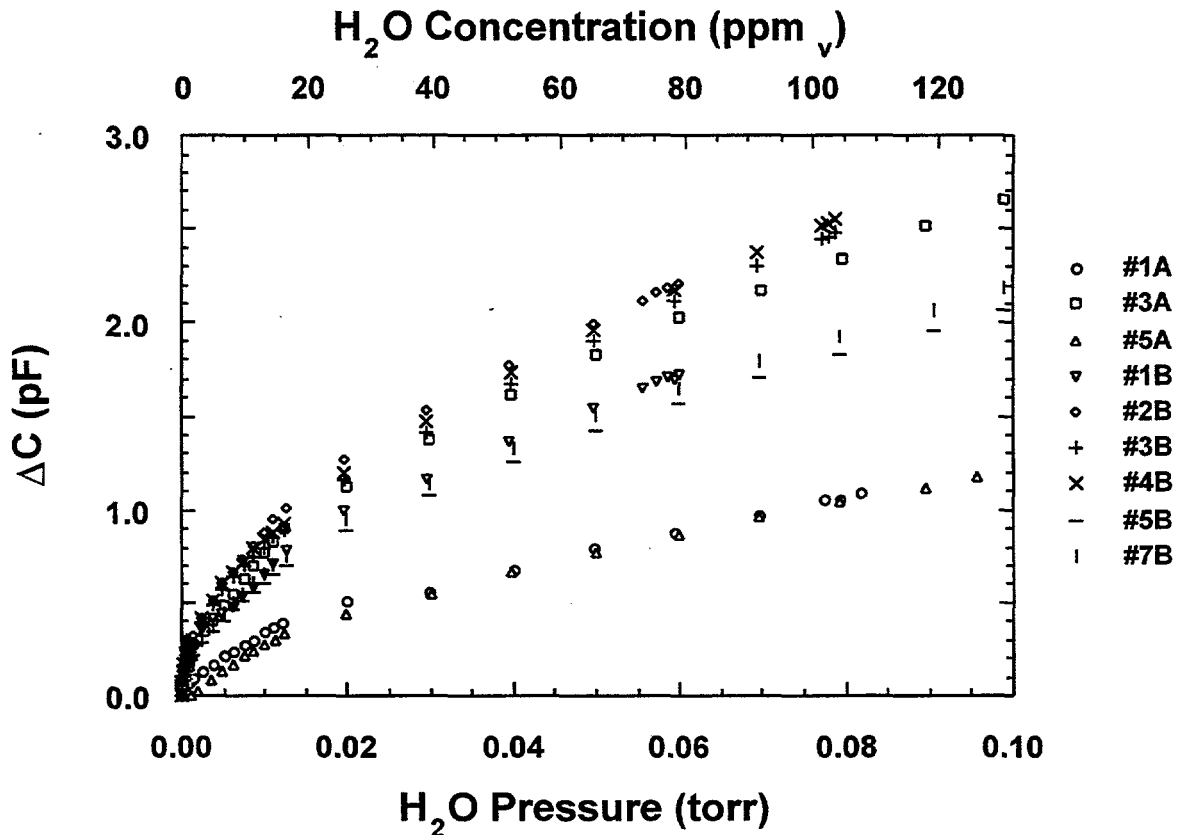


Figure 3: Variation in Moisture Sensitivity for a Series of PSC Sensors

relationship between output signal and H₂O pressure. However, variation in sensitivity is evident. Sensors 2B, 3A, 3B and 4B yield a 2.5 pF change for a background to 80 mtorr change in H₂O pressure. This behavior contrasts with the 1.8 pF change observed for sensors 5B and 7B and the 1.0 pF change observed for sensors 1A and 5A over this same pressure range.

Estimates of the sensitivities can be extracted from the data shown in Figure 3. Despite the fact that the data is non-linear over the entire pressure range, we note that near-linear behavior exists over individual, smaller pressure regimes. A sensitivity value can be extracted by calculating the tangent of the response curve for these regions using a least squares approximation. We have arbitrarily segmented the data into decade pressure regions to allow for sensitivity calculations. The results of this analysis are displayed in Table 1. The uncertainty in the calculated sensitivity values has been estimated by assuming that a combination of statistical and instrumental uncertainties contribute to the net uncertainty. We have followed the estimation method outlined by Bevington [5]. Sensitivity values are reported relative to both pressure and relative concentration with respect to volume for convenience. Note that true relative concentrations are not created in these experiments because H₂O is being investigated as a single component. Relative concentrations are calculated by referencing the absolute H₂O concentration present at a given pressure to that of a second constituent gas at 760 torr.

The data of Table 1 show that there is considerable variation in the pressure-dependent sensitivities for these sensors. Sensitivities vary from 10 to 25 pF/torr (0.008 to 0.019 pF/ppm_v), 28 to 65 pF/torr (0.021 to 0.050 pF/ppm_v) and 54 to 243 pF/torr (0.041 to 0.185 pF/ppm_v) in the 10 to 100 mtorr, 1 to 10 mtorr and 0.1 to 1 mtorr ranges, respectively. These distributions of sensitivity represent an approximate two-fold variation in sensitivity at the highest pressure range and an approximate four-fold variation at the lowest pressure range. Based on this data, calibration of individual sensors within a production lot will be required for quantitative moisture measurement. Note that the sensitivity is observed to decrease by a factor of two to four times for each subsequent increase in decade pressure range. This trend continues up to 1 torr pressures where sensors 3B, 4B, 5B and 7B were found to yield sensitivities of 4.96, 4.86, 5.83 and 5.92 pF/torr, respectively (not shown in Table 1). The consistency of these graduated pressure sensitivities demonstrate that the functional form of the sensors' response to H₂O is essentially constant within a given production lot.

Table 1: Variation in PSC Sensitivity and Lower Limit of Detection

Sensor	LLD (mtorr, ppb _v)	Sensitivity, 0.1-1 mtorr (pF/torr, pF/ppm _v)	Sensitivity, 1-10 mtorr (pF/torr, pF/ppm _v)	Sensitivity, 10-100 mtorr (pF/torr, pF/ppm _v)
1A	0.1, 130	54±5, (41±4)x10 ⁻³	28.0±0.5, (21.3±0.4)x10 ⁻³	10.03±0.06, (7.62±0.05)x10 ⁻³
3A	0.1, 130	168±13, (128±10)x10 ⁻³	59.7±0.6, (45.3±0.5)x10 ⁻³	20.53±0.07, (15.60±0.05)x10 ⁻³
5A	0.7, 900	-----	31.1±0.6, (23.6±0.5)x10 ⁻³	10.48±0.05, (7.96±0.04)x10 ⁻³
1B	0.1, 130	206±4, (157±3)x10 ⁻³	41.6±0.4, (31.6±0.3)x10 ⁻³	19.68±0.06, (14.96±0.05)x10 ⁻³
2B	0.1, 130	243±6, (185±5)x10 ⁻³	65.3±0.5, (49.6±0.4)x10 ⁻³	24.9±0.1, (18.9±0.1)x10 ⁻³
3B	0.1, 130	215±5, (163±4)x10 ⁻³	62.6±0.6, (47.6±0.5)x10 ⁻³	23.54±0.05, (17.89±0.04)x10 ⁻³
4B	0.1, 130	236±5, (179±4)x10 ⁻³	63.8±0.4, (48.5±0.3)x10 ⁻³	24.03±0.04, (18.92±0.03)x10 ⁻³
5B	0.05, 65	115±4, (87±3)x10 ⁻³	47.0±0.5, (35.7±0.4)x10 ⁻³	16.35±0.04, (12.43±0.03)x10 ⁻³
7B	0.05, 65	137±6, (104±5)x10 ⁻³	51.5±0.6, (39.1±0.5)x10 ⁻³	17.11±0.09, (13.00±0.07)x10 ⁻³

Lower limits of detection (LLD) of these sensors can be estimated based on the pressure that produces the first significant response above the C_b value. Significance is determined by the precision of the capacitance measurements. Our capacitance measurements are made at a resolution of 0.01 pF. Short term stability tests (one hour or less) show that a sensor will yield a capacitance value with an uncertainty of ± 0.01 pF. Adopting the convention that a signal-to-noise ratio of two is required for statistical significance, a 0.02 pF change is considered the smallest meaningful change. Figure 4 shows the response of sensor 5B to a 5×10^{-5} torr H_2O pressure step from a 6×10^{-8} torr base pressure. The sensor responds slowly to this pressure increase and eventually yields a stable change in capacitance of 0.07 pF after 3600 seconds of equilibration. This data demonstrates that this sensor will respond to H_2O levels at less than 5×10^{-5} torr or 65 ppb_v. We also note that a 0.02 pF change is observed in a single 68 second sample period after initiation of this pressure increase. This result indicates that the sensor will respond to as little as 3.4×10^3 L (1 Langmuir = 10^{-6} torr-sec) of H_2O exposure, despite these response time constraints.

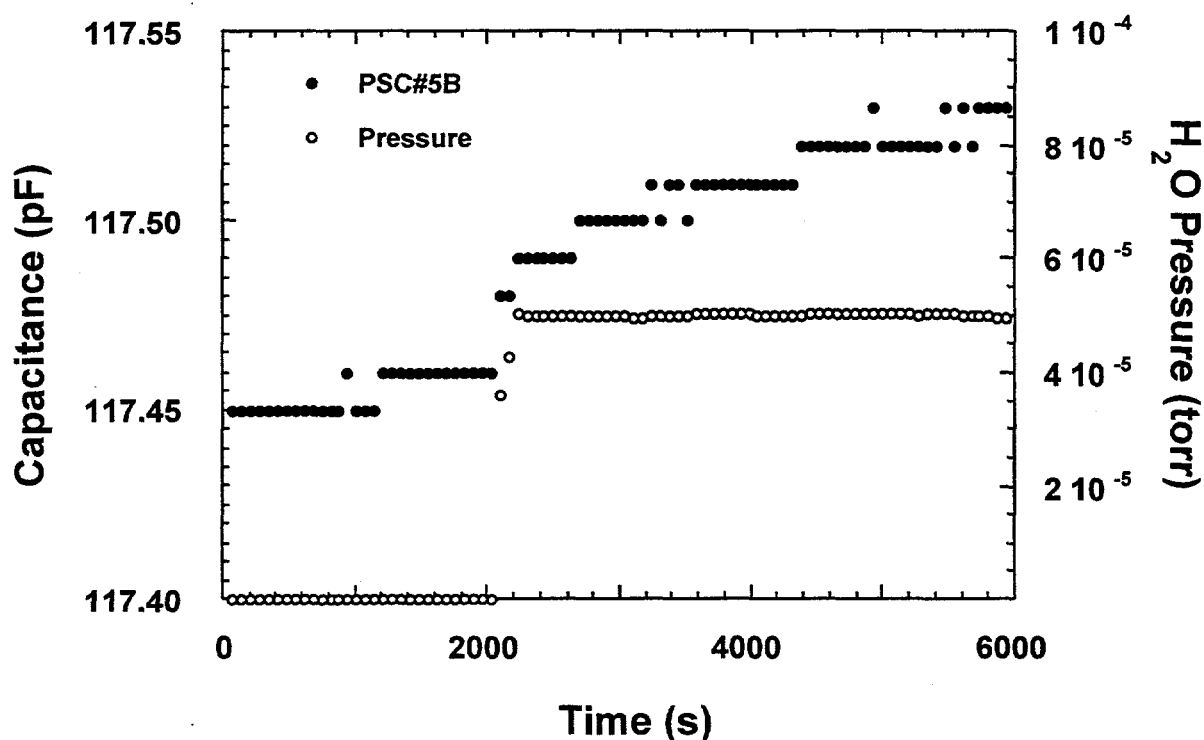


Figure 4: Response of PSC #5B to 5×10^{-5} torr H_2O Pressure Step

Estimates of the LLD are dependent on the initial condition of the sensor and the conditions of the experiment used to measure this value. The sensor must be dry, yielding a minimum C_b value, to show a response at low pressures. The first pressure step in a calibration sequence must be sufficiently small in magnitude and long in duration to allow measurement of the LLD. The values displayed in Table 1 reflect variations in measurement process more than variations in sensor response. As a result, the minimum LLD value of 65 ppb_v is our most reliable estimate of

the intrinsic LLD for this sensor lot. Whether this intrinsic detection limit can be taken advantage of will be dependent on the applications environment.

III.3 Sensor Stability

The stability of the capacitance of a sensor at a particular moisture level will be determined by drift in the C_b value. Therefore, it is important to understand how the dry response of the sensor varies with time. We have observed long term drift in these sensors over periods of several hours to several weeks. The greatest contributor to long term drift is the slow drying of the sensor, as will be discussed in Section III.6 of this report. To determine long term stability, we monitored the C_b value of a pair of sensors over a 38 day period. These results are summarized in Table 2.

Table 2: Long Term Drift in PSC Baseline Capacitance

Time * (days)	#3B C_b (pF)	#4B C_b (pF)
3	115.38	116.51
10	114.97	116.25
26	114.92	116.26
31	114.73	116.01
38	114.74	116.12

* Time after vacuum installation of the sensor

The data of Table 2 show that over the course of a 38 day period, a gradual decrease in C_b was observed. A maximum change of 0.64 and 0.5 pF was observed for sensors 3B and 4B, respectively. Over this 38 day period, the chamber was vented, baked and backfilled with H_2O up to levels of 1000 ppm_v. The data in Table 2 represent capacitance values of the sensors after having sat at the chamber base pressure for a period of at least 70 hours. These values of C_b should represent the dry response of these sensors. The maximum changes in C_b can be thought of in terms of H_2O concentration measurement errors because measurement of capacitance is made with respect to an assumed constant C_b value. Based on the initial calibration data for these sensors, we find that drift creates an error of 5 and 2 ppm_v for sensors 3B and 4B, respectively. The consequence of drift is to significantly increase the probable error of a sensor's measured moisture level.

A second concern involving PSC stability is variation in the sensitivity with time. We have conducted a limited amount of testing to evaluate whether sensitivity varies over an extended period of vacuum containment. Sensors 5B and 7B showed no discernible change in sensitivity for two calibrations initiated 40 and 110 hours after vacuum installation. This result suggests there are no short term variations in sensitivity. We have also monitored changes in sensitivity for sensors 3B and 4B over a 30 day period. The results of these tests are shown in Table 3. This data shows that changes in sensitivity do occur over longer periods of time. We observe an approximate 23% decrease in sensitivity between calibrations conducted 3 and 12 days after vacuum installation. Sensitivity values generated after 30 days in vacuum show no change for sensor 3B while sensor 4B shows an additional 10% decrease. The sensors were subjected to a number of atmospheric venting and chamber heating cycles between calibrations. These venting and heating cycles raise concerns that sensitivity changes could be produced by contamination. As will be discussed in Section III.4, the C_b value is a sensitive indicator for hydrocarbon

contaminant uptake. The small decreases observed in the C_b values of Table 3 suggest that contamination is not the source of this sensitivity decrease. It is unclear if this gradual decrease in sensitivity is a consistent characteristic of these sensors based on our experiments. If it is, it may indicate an aging effect where either changes in the porous Si dielectric or changes at the electrode/dielectric interface govern the eventual sensor response.

Table 3: Long Term Variation in PSC Moisture Sensitivity

Time* (days)	#3B C_b (pF)	Sensitivity, 1-10 mtorr (pF/torr, pF/ppm.)	#4B C_b (pF)	Sensitivity, 1-10 mtorr (pF/torr, pF/ppm.)
3	115.38	62.6±0.6, (47.6±0.5)×10 ⁻³	116.51	63.8±0.4, (48.5±0.3)×10 ⁻³
12	114.97	48.2±0.5, (36.6±0.4)×10 ⁻³	116.25	48.8±0.5, (37.1±0.4)×10 ⁻³
30	114.73	47.8±0.5, (36.3±0.4)×10 ⁻³	116.01	43.8±0.5, (33.3±0.4)×10 ⁻³

*Time after vacuum installation of sensor

III.4 Contaminant Effects on Sensor Response

The PSC moisture detection scheme is based on adsorption. The porous Si matrix is not a selective adsorbent which leads to the possibility of competitive adsorption between H₂O and contaminants. Any adsorbate that is polarizable can contribute to the overall capacitance change. In the SIV system, mechanical pump oil is the primary contaminant available for competitive adsorption by the sensor. It is anticipated that many of the potential vacuum applications of the PSC will involve mechanical pumping schemes and the possibility of trace oil exposure. The SIV system uses a high compression ratio turbomolecular pump separated from a two stage rotary vane pump by a molecular sieve trap. Normal operation of the system places the level of oil contamination below 1×10⁻⁹ torr based on mass spectrometric and ion gauge measurements. However, we experienced a system failure where the sorption trap was heated during a system bake yielding a detectable quantity of hydrocarbon contamination. We estimate an exposure of the sensor of 0.35 torr for 3300 seconds at 100°C. This event occurred at the end of our evaluation period for sensors 3B and 4B. The decision was made to evaluate the effect of this contamination on sensor C_b and sensitivity.

Oil contamination produces a dramatic shift in the C_b value with only a moderate effect on the PSC's moisture sensitivity. We have measured a shift of 114.73 to 130.15 pF and 116.12 to 126.98 pF for sensors 3B and 4B, respectively. This shift is essentially permanent. Attempts to bake the system eventually eliminated detectable quantities of hydrocarbon in the vacuum environment but never produced a return to original C_b values for the sensors. The sensors remain active to moisture, although the sensitivity does decrease. Figure 5 shows a comparison of the calibration plots for sensor 3B prior to and after oil exposure. These data show that the functional form of the sensor response has not been dramatically changed with hydrocarbon contamination. Table 4 contains the calculated sensitivities for the pressure ranges studied. We find that the sensitivity has decreased approximately by a factor of two for pressures above 1 mtorr. Sensor 3B shows a 26% decrease in sensitivity for pressures below 1 mtorr while sensor 4B shows a 31% increase. The increased sensitivity shown by sensor 4B at low pressures is difficult to explain. We can, however, explain the overall retention of sensitivity at low pressures along with the degradation at higher pressures. The role of a co-adsorbed hydrocarbon would be

to make regions of the porous structure hydrophobic on a local scale. The hydrocarbon effectively decreases the total area available for H₂O adsorption. However, the hydrocarbon would not be attracted to the same adsorption sites that are active toward H₂O. In fact, the more active a site is for H₂O the less likely a hydrocarbon would be expected to be irreversibly bound.

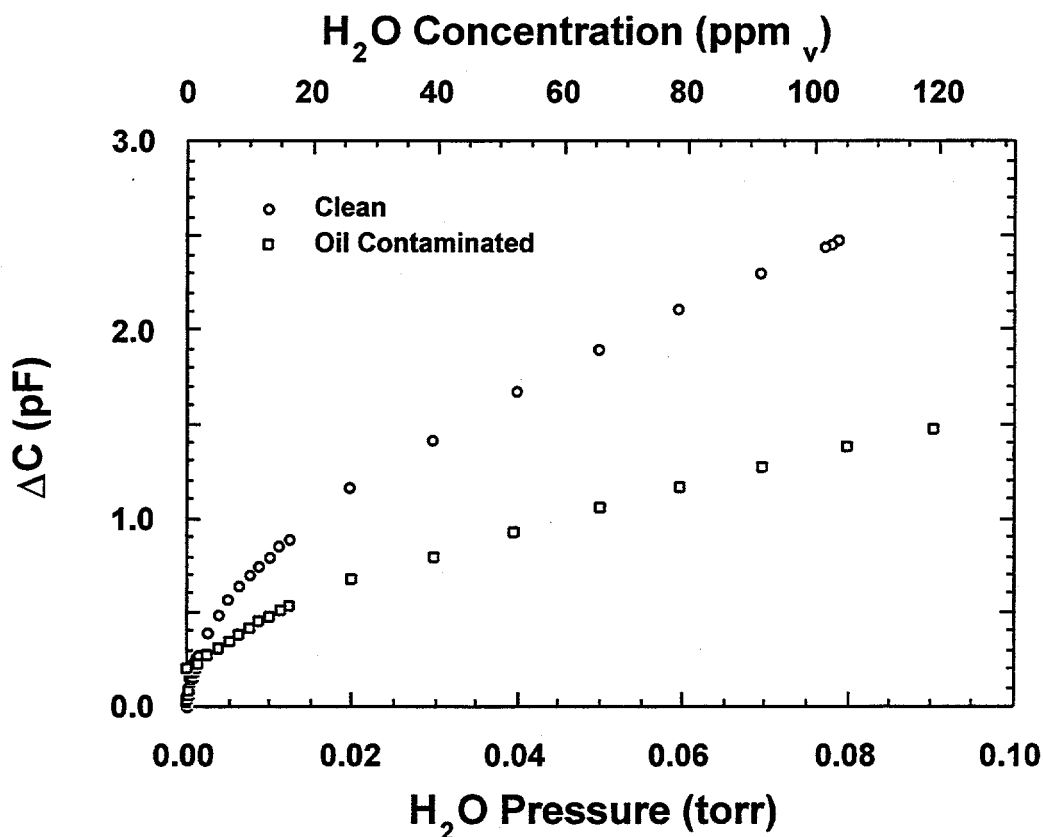


Figure 5: Effect of Hydrocarbon Contamination on PSC Response

Table 4: Impact of Hydrocarbon Contamination on PSC Sensitivity

Sensor	Condition	Sensitivity, 0.1-1 mtorr (pF/torr, pF/ppm _v)	Sensitivity, 1-10 mtorr (pF/torr, pF/ppm _v)	Sensitivity, 10-100 mtorr (pF/torr, pF/ppm _v)
3B	clean	236±5, (179±4)×10 ⁻³	63.8±0.4, (48.5±0.3)×10 ⁻³	24.03±0.04, (18.92±0.03)×10 ⁻³
3B	oil	175±5, (133±4)×10 ⁻³	29.8±0.4, (22.6±0.3)×10 ⁻³	10.85±0.04, (8.25±0.03)×10 ⁻³
4B	clean	215±5, (163±4)×10 ⁻³	62.6±0.6, (47.6±0.5)×10 ⁻³	23.54±0.05, (17.89±0.04)×10 ⁻³
4B	oil	282±5, (214±4)×10 ⁻³	29.8±0.6, (22.6±0.5)×10 ⁻³	9.32±0.05, (7.08±0.04)×10 ⁻³

This site selective interaction should result in preservation of the more active sites populated by H₂O at low pressures. The net effect of the hydrocarbon would then be to physisorb at low polarity adsorption sites thus impeding large scale multilayer adsorption and condensation.

III.5 Sensor Response Time Characteristics

The PSC sensor response time can be evaluated by monitoring the time-dependent response of capacitance with a pressure increase. This information is available in the calibration experiments where a controlled pressure increase with time is produced. Figures 6a and 6b show the lower exposure response of sensors 3B and 5B subjected to slightly different pressure waveforms. Sensor 3B was taken from a dry state to 1×10^{-4} torr and allowed to sit for 30 minutes followed by exposure to 30 minute increments of 1×10^{-4} torr. Sensor 5B was taken from a dry state to 5×10^{-5} torr for 60 minutes and then treated identically to sensor 3B. The data show several interesting exposure related trends in both magnitude and rate of capacitance change. Both sensors show the largest change in absolute capacitance for the first few steps. Further increases in exposure show a decreased capacitance change. Sensor 3B shows a constant signal change during each of the first three steps with signal equilibration occurring only after the fourth step. In contrast, sensor 5B shows signal equilibration after the second step. As a class, all of the sensors show this same general trend; a disproportionately large signal change can be produced with low level exposure and signal equilibration is a function of exposure time. This combination of magnitude and rate of change information argues that the PSC exhibits slow

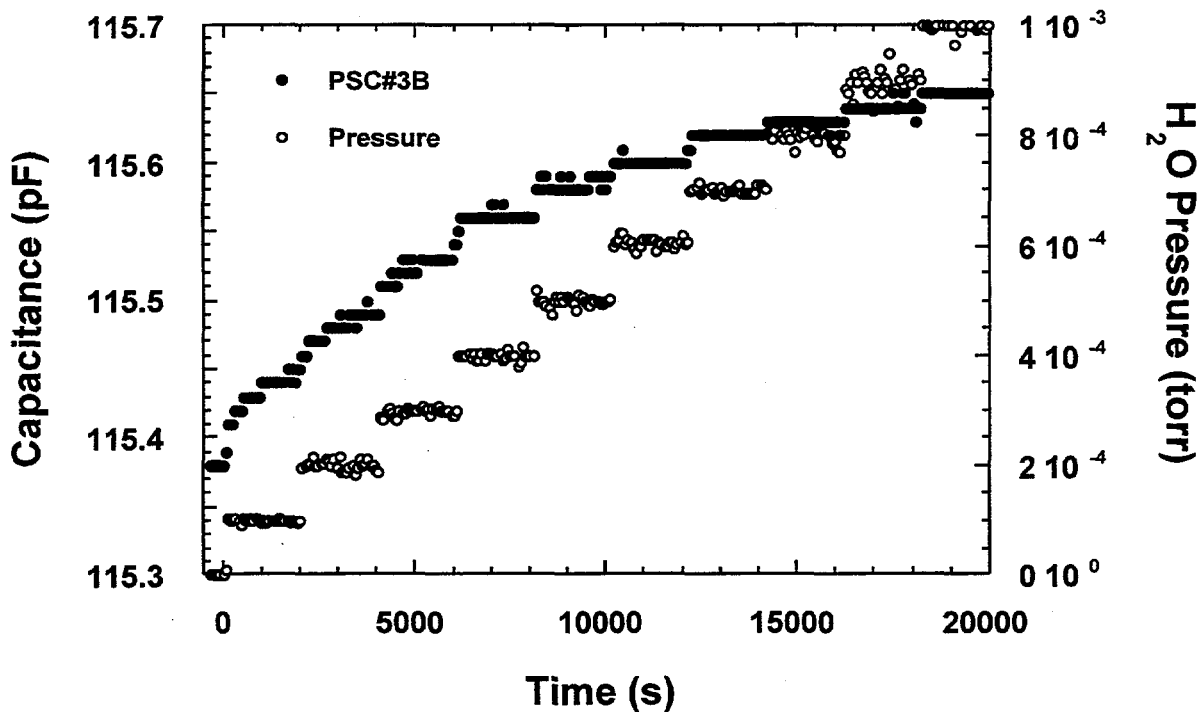


Figure 6a: Low Pressure Response of PSC Sensor #3B

adsorption kinetics at low moisture levels. If we assume that the capacitance is proportional to adsorbed H₂O quantity at low exposure, this disproportionate change can be interpreted as a titration of the most active adsorption sites. The attenuated capacitance change observed after this saturation process signals a distinction between irreversible and reversible adsorption regimes.

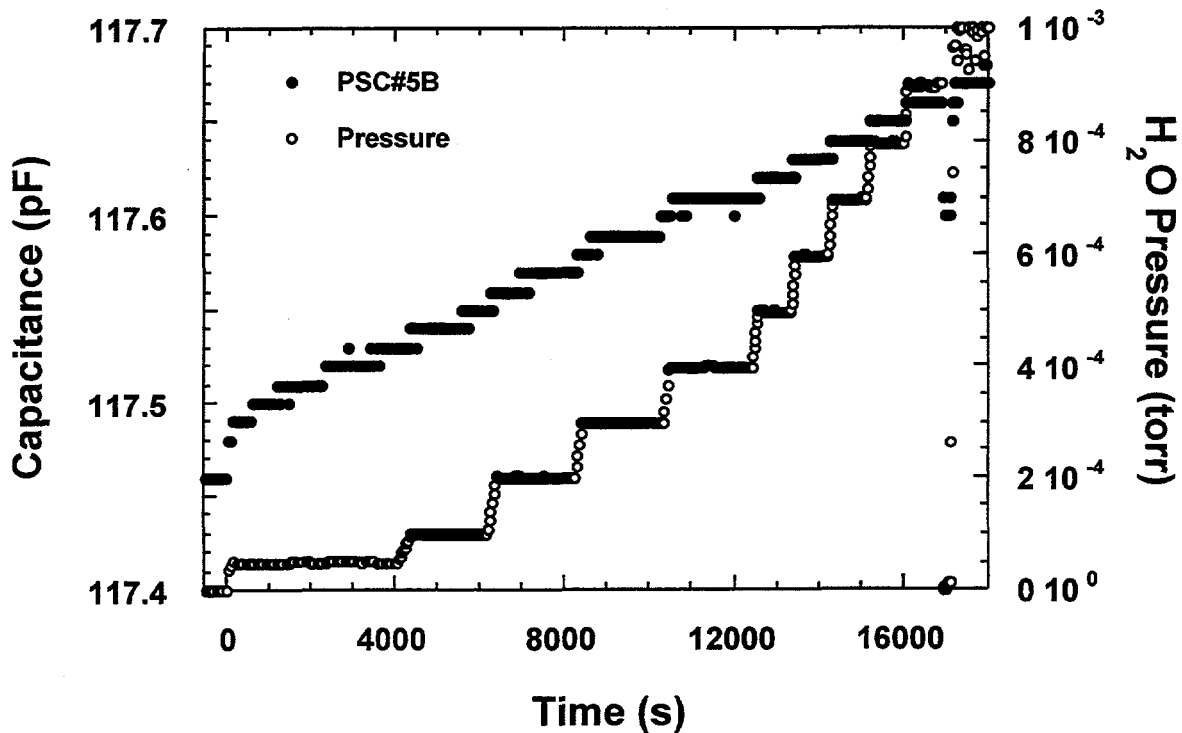


Figure 6b: Low Pressure Response of PSC Sensor #5B

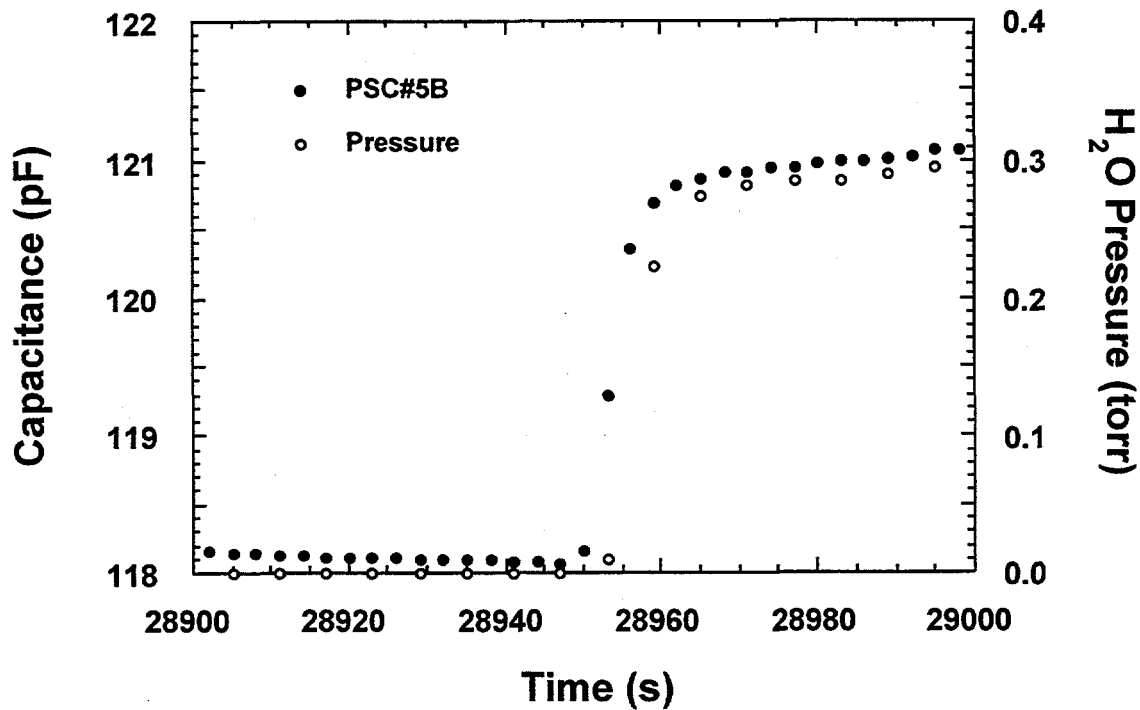


Figure 7: Response of PSC #5B to a 3 × 10⁻¹ torr H₂O Pressure Step

Sensor response times are a function of exposure conditions. The data of Figure 4 indicate that sensor 5B exhibits a response time of 3600 seconds for exposure to 5×10^{-5} torr H_2O . Equilibration becomes much more rapid at higher moisture levels. Figure 7 shows the response of sensor 5B to a pressure step from 3×10^{-4} to 0.3 torr. The sensor tracks the pressure change within the limits of sampling interval indicating that the response time is on the order of 8 seconds at this higher pressure. This increase in adsorption rate is expected at higher pressures due to the greater rate of mass transport.

This variation in response time with exposure can be evaluated in a more quantitative fashion. We subjected sensor 1A to a series of sequential pulses from a background pressure of 1×10^{-7} torr to 0.1, 1, 10 and 100 mtorr. The sensor's response to the leading edge of each of these pulses is shown in Figure 8. This experiment is different from the pressure step (calibration)

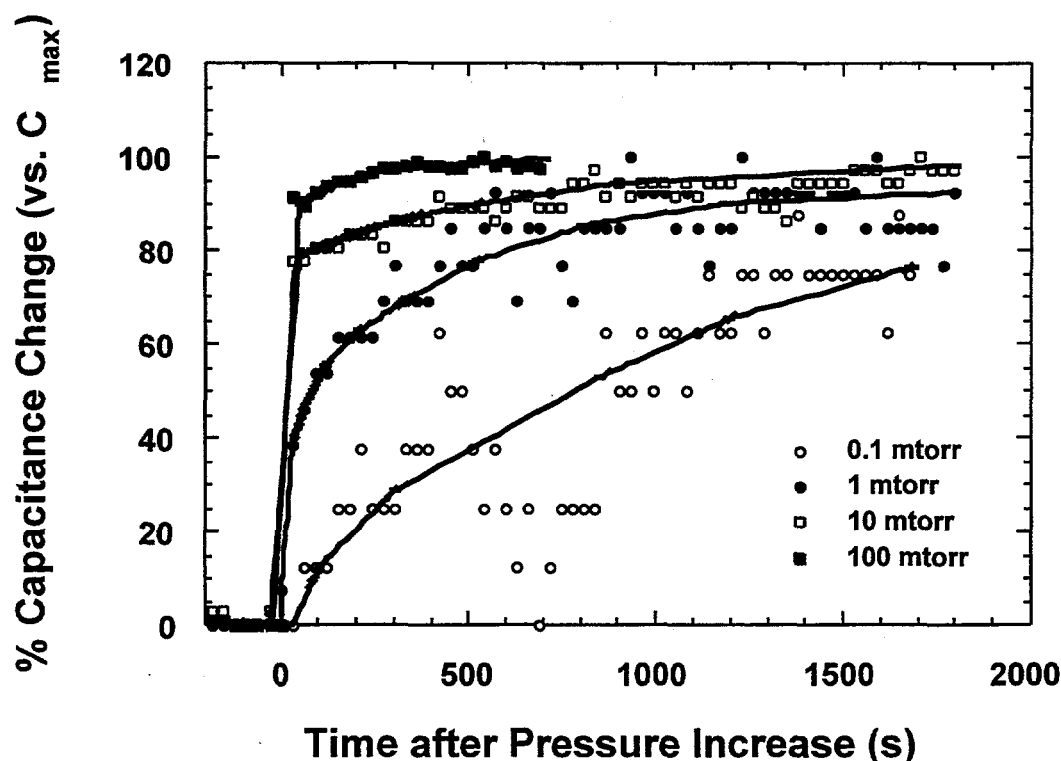


Figure 8: Response Time Characteristics of PSC #1A with H_2O Pressure Increase: labels denote final H_2O pressure, initial H_2O pressure $< 1 \times 10^{-7}$ torr.

procedure in that the sensor is allowed to dry for 1800 seconds at 1×10^{-7} torr after each pulse. The observed response for sensor 1A is typical of this class of sensors. At 0.1 mtorr, the sensor requires a period of ~ 2000 seconds to yield a signal that is 80% of the eventual maximum output (C_{max}). Extended measurements at 0.1 mtorr show that times on the order of an hour are required for equilibration of sensor 1A. With increased exposure, the times required for achieving 80% of the eventual maximum signal decrease to 700, 30 and < 30 seconds for 1, 10 and 100 mtorr pulses, respectively. This decreased response time with exposure is consistent with that observed in the previously discussed step data. It is interesting to note that the response time does not scale directly with pressure as expected; we would expect a 10 fold decrease in equilibration time with

a 10 fold increase in pressure. This observation suggests that other mechanisms of mass transport (i.e. surface diffusion, transitional flow, etc.) are responsible for positioning H₂O at the active adsorption sites within the porous structure.

The rate at which the sensor responds to pressure reduction is of equal importance when discussing response times. The pressure reduction response time can be evaluated in much the same way as the pressure increase times displayed in Figure 8. A similar set of pressure pulses were used with a suitable time period allowed for a return to a background pressure between pulses. The results of this experiment are shown in Figure 9 for sensor 5A. Four pulses of 0.1, 1, 10, and 100 mtorr at 2100 seconds were used separated by a 2100 second return to a baseline pressure of 2×10^{-7} torr. In this experiment, the vacuum system required only 100 seconds to transition from 100 mtorr H₂O to a baseline pressure of less than 1×10^{-6} torr. For all of these exposures, we find that the sensor does not completely return to its C_b value of 120.61 pF after several thousand seconds of evacuation, indicating a slow drying of the sensor. The sensor yields values of 0.02%, 0.02%, 0.08% and 0.2% of C_b 2100 seconds after exposure to 0.1, 1, 10 and 100 mtorr H₂O, respectively. These values correspond to deviations from C_b of 0.02, 0.1 and 0.24 pF. The extent to which the sensor recovers to its baseline value scales inversely with exposure. The fact that the evacuation responses for both 0.1 and 1 mtorr exposures both yield 0.02 pF deviation is consistent with irreversible adsorption at lower pressures as discussed previously. After a 100 mtorr exposure and 4400 seconds of evacuation, the sensor has recovered to only within 0.12% of its C_b value. Based on the calibration data for this sensor, we find that a 0.14 pF deviation from C_b corresponds to an absolute error of 6 mtorr. This value represents a significant degree of error and reflects the degree to which the slow response of these sensor impacts

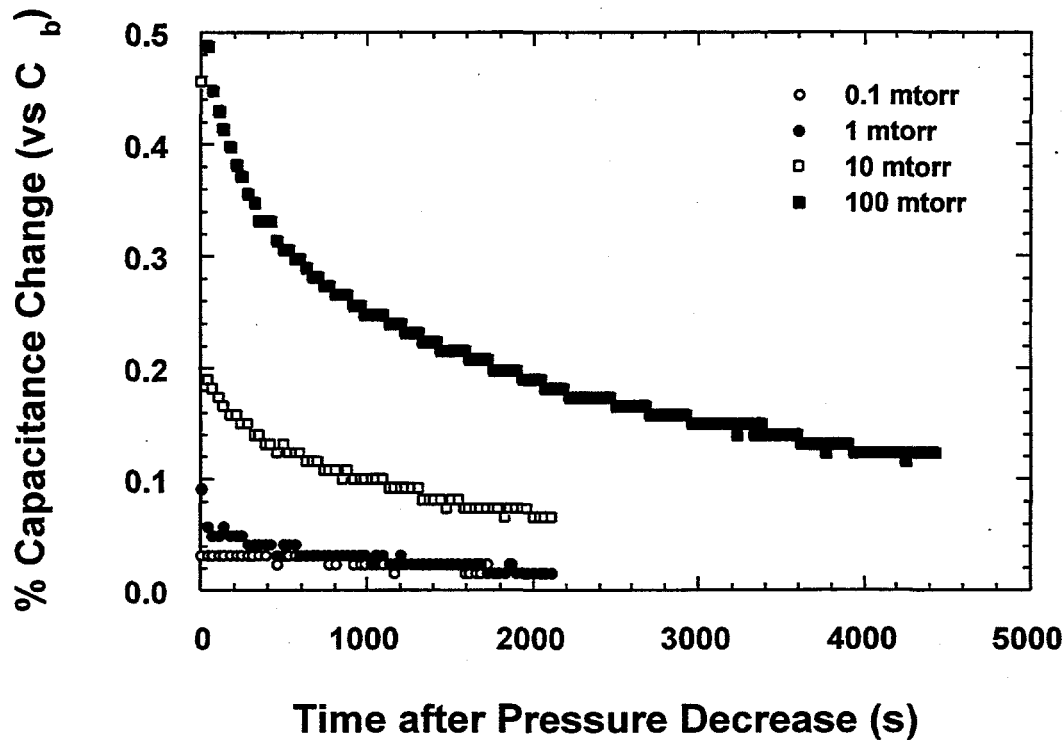


Figure 9: Response Time Characteristics of PSC #5A with H₂O Pressure Decrease: labels denote initial H₂O pressure, final H₂O pressure $< 2 \times 10^{-7}$ torr.

quantitative moisture measurements for dynamic environments.

These response time measurements are instrumental in identifying the useful operational range of the PSC. We have found that the transition to rapid sensor equilibration (60 seconds or less) for pressure increases does not occur until H₂O pressures are in the mtorr regime. This property limits the use of the sensor for monitoring short term increases in H₂O pressure to levels above 1 mtorr. However, static system monitoring could be extended to pressures below 1 mtorr. Any application of this sensor will also have to take into account the time necessary for the sensor to dry to a level where a meaningful measurement can be made. We have found that the time required for the sensor to dry is on the hour time frame and errors as large as 6 mtorr can result in moisture level measurements made prior to complete drying. The rate at which the sensor dries is determined by how H₂O escapes from the porous structure and is the focus of the following vent studies.

III.6 Simulated Vent Test Results

The PSC sensor has been considered as a candidate device for monitoring moisture levels in load lock operations. The sensor's response to atmospheric exposure as well as the time required for complete drying are critical issues for this application. We have conducted a variety of tests designed to evaluate the sensor's response to high levels of moisture. These tests include atmospheric venting of the test chamber, simulated venting using controlled H₂O pressures and repetitive atmospheric exposures to evaluate the reproducibility of response characteristics. Atmospheric vent and evacuation procedures represent the first point in our experiments where the H₂O partial pressure cannot be measured using the total pressure standard gauges. H₂O partial pressure will be dictated by the relative humidity of the laboratory ambient atmosphere once the equilibrium is achieved in the chamber with venting. Under these conditions, the relative humidity (RH) will dictate H₂O pressure which will be some fraction of the chamber pressure. Chamber venting and evacuation are non-equilibrium processes and significant disparities in true and RH-derived H₂O pressures are expected. The chamber pressure reflects an upper limit for the H₂O pressure under non-equilibrium conditions.

The overall response of a PSC sensor to an atmospheric vent is quite fast. A representative response curve is shown in Figure 10 where the calibrated response of sensor 3B is displayed as a function of time. The chamber pressure has also been included to allow for direct comparison. The multi-step character of these traces is a result of the fact that the chamber cannot be vented instantaneously. This limitation provides additional justification for using regulated H₂O pressure pulses to evaluate sensor response times. The data of Figure 10 show that the sensor response tracks the chamber pressure. We find a 150 second delay for the sensor with vent initiation at 750 seconds, consistent with the slow equilibration at low pressures as previously discussed. The sensor starts responding on a time scale of 30 seconds (the sampling interval) as the chamber pressure exceeds 10 mtorr. This 30 second response time is maintained for pressures up to 630 torr where the sensor response limits at 3 torr of H₂O. We estimate that typical relative humidity (RH) values in the laboratory range from 10 to 20%. At a nominal atmospheric pressure of 630 torr, this RH range places the H₂O partial pressure between 2 and 4 torr. The reported PSC measurement of 3 torr is consistent with these estimates.

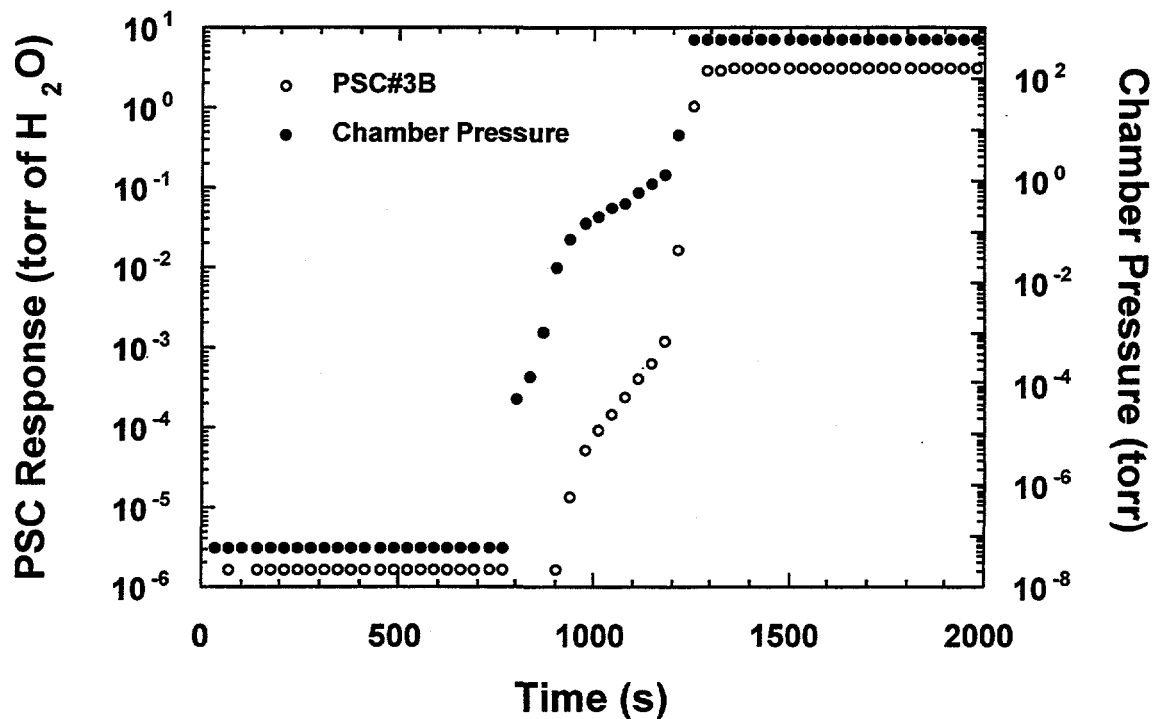
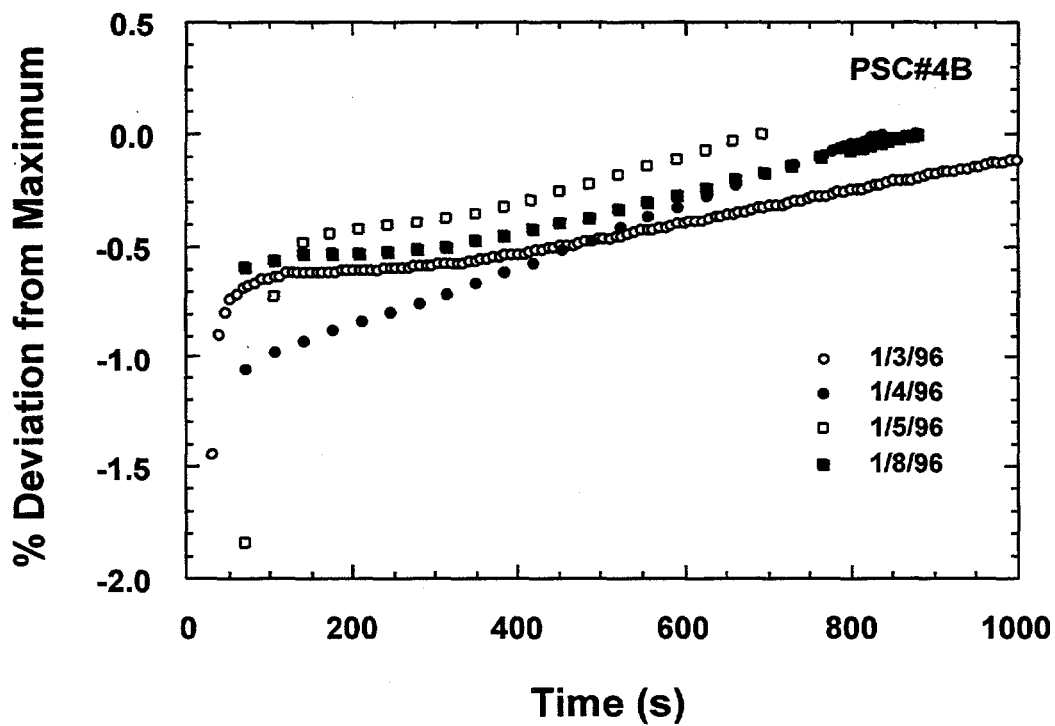
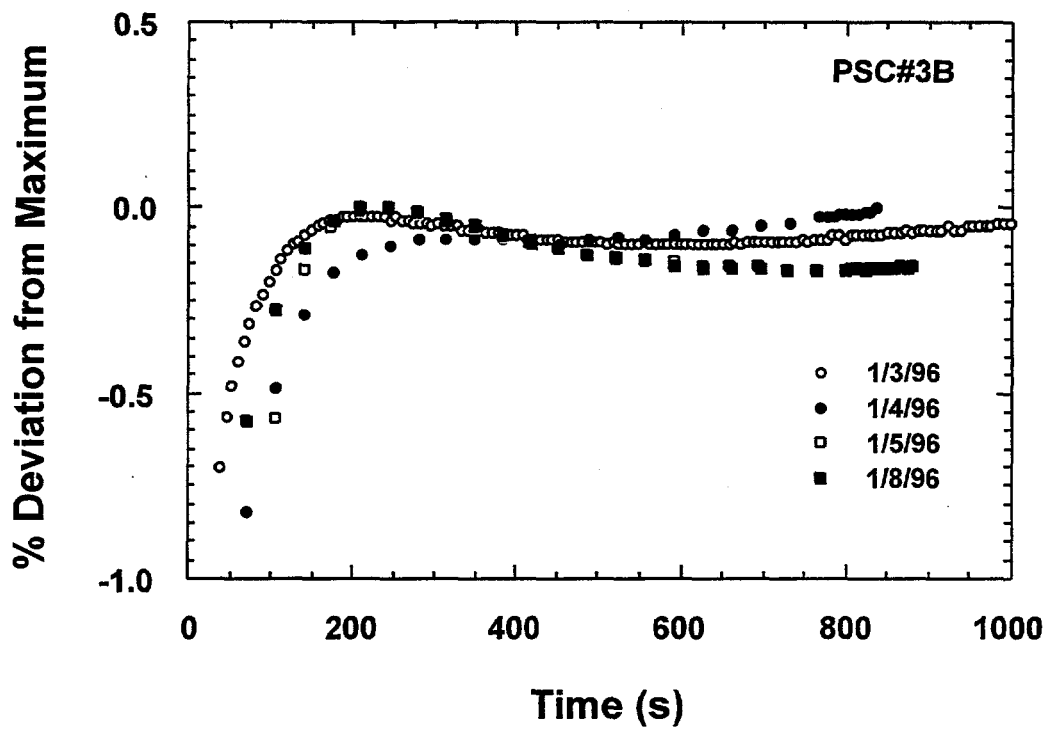


Figure 10: Variation in PSC #3B Calibrated Response and Chamber Pressure as a Function of Atmospheric Venting

Some degree of signal variation is observed over short term atmospheric exposure. The time-dependent responses of sensors 3B and 4B are shown in Figures 11a and 11b. Capacitance values have been converted to a percent deviation from the maximum value observed during exposure. This conversion allows for comparison of a sensor's response despite daily variations in room humidity. These two sensors show significantly different responses when simultaneously subjected to atmospheric exposure. Sensor 3B shows an initial maximum in signal with venting followed by an approximate 0.1% decrease and a subsequent gradual increase in signal over the first 800 seconds of exposure. In contrast, sensor 4B shows a continual, slow rise in signal of 0.5 to 1.0% over this same time period. It is also noted that the day-to-day variation in signal response has the same approximate functional form for a given sensor. These results demonstrate that sensors can be expected to respond differently to constant exposures of humidity at high levels. We can also conclude that, despite these differences, signal variation is an intrinsic property of the sensor and is reproducible. The gradual rise in signal for sensor 4B may be related to slow equilibration of a conductance restricted portion of the porous Si layer. This interpretation suggests structural heterogeneity is created during the fabrication of these sensors.



Figures 11a & 11b: Time-Dependent Responses of PSC #3b and #4B to Atmospheric Exposure:
number label indicates date of experiment

The PSC sensors recover slowly from atmospheric venting. Figure 12 shows the variation in the calibrated response of sensor 3B and the chamber pressure with evacuation after 15 minutes of atmospheric exposure. Evacuation was initiated at 2100 seconds and an 8 second sampling interval was used. The data show that the sensor signal drops from 3 to $\sim 5 \times 10^{-2}$ torr H₂O during the first 100 seconds of evacuation. The chamber pressure decreases from 630 to $\sim 1 \times 10^{-5}$ torr during this same time period. The relative magnitudes of the PSC and chamber pressures allows an estimate of probable error in the PSC measurement of approximately 50 mtorr at 100 seconds after evacuation. This disparity in the calibrated PSC response and total pressure values indicates a slow drying of the sensor. This slow drying is confirmed by the gradual decay of the PSC signal observed for times longer than 2200 seconds. The probable error decreases to only 30 mtorr for times approaching 1000 seconds. This stage represents the slow release of H₂O from the porous structure and sets a limit for the time necessary for complete drying of the sensor. Continued monitoring of the sensor for times longer than 3000 seconds (not shown in Figure 12) demonstrated that a return to C_b requires a period in excess of 22 hours. Despite the variations observed in the time-dependent sensor response with atmospheric exposure, sensors 3B and 4B show essentially identical evacuation responses. This similar drying behavior is most likely a result of the fact that complete drying requires so much time that subtle differences in maximum adsorption capacities and conductance rates (as seen in Figure 11a and 11b) are not visible during evacuation and desorption.

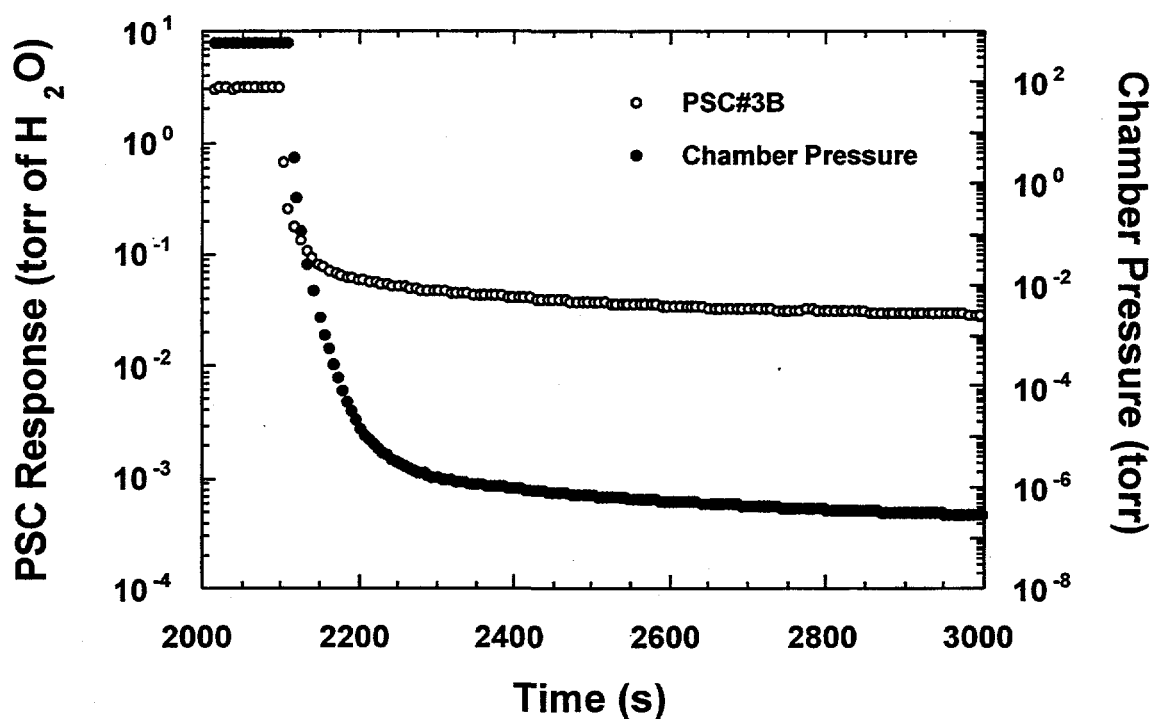


Figure 12: Variation in PSC #3B Calibrated Response and Chamber Pressure as a Function of Atmospheric Evacuation

The slow drying of these sensors raises questions concerning whether precise, absolute moisture measurements can be made with a PSC. We have monitored a set of sensors for as long as 74 hours after exposure and evacuation and have found that a full return to a C_b value is possible. This result is illustrated in Figure 13 where the difference, ΔC , between the measured and baseline capacitance of sensor 4B is shown as a function of time after evacuation. Approximately 70 hours are required for the sensor to return to its C_b value. This result indicates

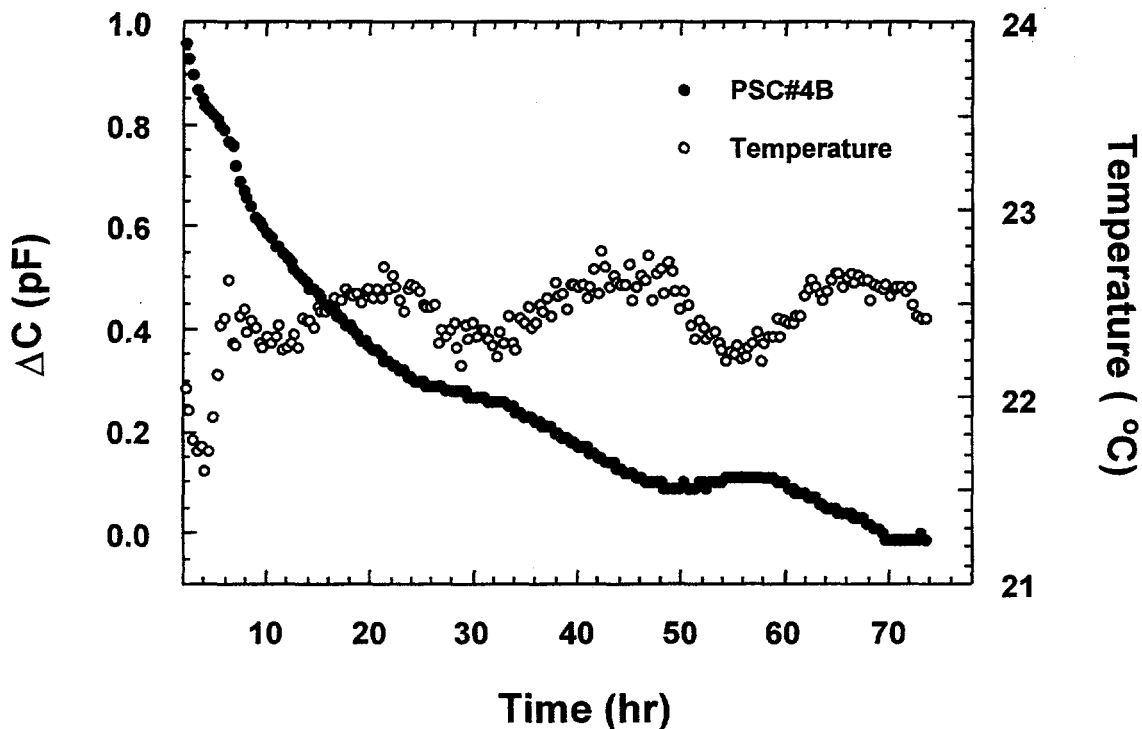


Figure 13: Long Term Response of PSC #4B to Evacuation

that capacitance values can be referenced to a C_b value provided ample time exists for adequate drying.

The data of Figure 13 also suggest that the PSC sensor is susceptible to small scale thermal variations. Superimposed on the continuous capacitance decay is a cyclic variation that appears to correlate with variations in the system temperature. Temperature measurements were made on the rotor housing of the spinning rotor gauge. The initial temperature rise observed between 2 and 6 hours is a result of re-warming of the rotor housing after having cooled during evacuation due to H_2O vaporization. The sensor does not see this local thermal trend. The remaining cycles in the temperature profile have a period of 24 hours and correspond to heating and cooling of the room. The PSC appears to be responding to these cycles. Assuming that adequate drying has occurred 50 hours after evacuation, we find that as much as a -0.1 pF shift can occur for a +0.3 °C temperature change. Note that this trend implies that the sensor has a negative thermal coefficient at room temperature. This trend is in contrast to the observed positive thermal

coefficient observed over the 45 to 90_C temperature range. A thermally-induced variation in the C_b value will contribute a larger indeterminate error in a PSC moisture reading.

Thermal Heating of the PSC Sensor

We have demonstrated that the PSC sensor dries slowly and that any attempt to extract a quantitative measure of moisture can lead to significant measurement errors. One method for speeding up the drying process is to apply a thermal pulse to the device. We investigated the effect of thermal pulsing of the sensors by applying a 0.5 A current pulse at a limiting voltage of 20 V for one second. Our goal was to localize heat within the sensor and rely on the remainder of the Si die and the TO-39 header, on which the die is mounted, to act as a thermal sink for rapid cooling. The top Al grid electrode served as an integrated heater in this experiment. Using this approach, we typically observe a maximum 90_C transient as measured by an integrated, temperature-sensitive diode. We find that under these conditions a time period of greater than 15 minutes is required for complete cooling of the sensor (within +0.5_C).

Thermal pulsing of the sensor produces a significant improvement in signal recovery after H₂O exposure. The calibrated response of sensor 4B to evacuation after a 1 torr H₂O exposure (10³ torr-sec) with and without a thermal pulse is shown in Figure 14. The chamber H₂O pressure, as measured by the transfer standard gauges, is included for direct comparison. A control experiment where the dry sensor was subjected to an identical pulse is also shown. The thermal pulse was applied to the sensor 120 seconds after initiating evacuation. We found that the dry sensor responds to a thermal pulse with a signal increase due to heating followed by a gradual decay. The sensor requires a period of greater than 10 hours to return to a baseline response of $<5 \times 10^{-5}$ torr. This result is surprising given the fact that the sensor only requires 15 minutes to cool to within +0.5_C of initial temperature. This results suggests that the diode measurement may not be an accurate indication of the temperature in the porous region.

Evacuation after a 1 torr H₂O exposure produces a slow, exponential decay in sensor signal. The data show that 10 hours of evacuation produce a 5 mtorr reading on the PSC while the chamber H₂O pressure has decayed to 1×10^{-8} torr. This slow response of sensor 4B to a 1 torr H₂O exposure is nearly identical to that observed for an atmospheric exposure. We conclude that a 1 torr H₂O exposure is a reasonable simulation of atmospheric exposure. A second conclusion that can be drawn is that the PSC sensor is slow to recover from low level H₂O exposures, consistent with the expectation of conductance-limited transport of H₂O within the porous structure.

A thermal pulse produces measurable gains in the time-dependent response of the PSC sensor. The data of Figure 14 show that application of a thermal pulse produces a similar slow decay in PSC signal with a pressure reading of 2 mtorr at 10 hours. This compares to the value of 5 mtorr observed without heating and a chamber H₂O pressure of 1×10^{-8} torr. Heating also produces an improvement in short term (< 1 hour) response of the sensor. The data in Figure 14 show that as much as a 20 mtorr difference is observed between the two traces for the first hour after evacuation. The short term effect of the pulse is to flatten the decay at short times and produce a signal closer to the sensor's LLD. Given that thermal energy input to the sensor produces its own capacitance increase, the effective use of thermal energy to shift adsorption equilibrium may be best obtained by coupling both heating and cooling capabilities. The goal

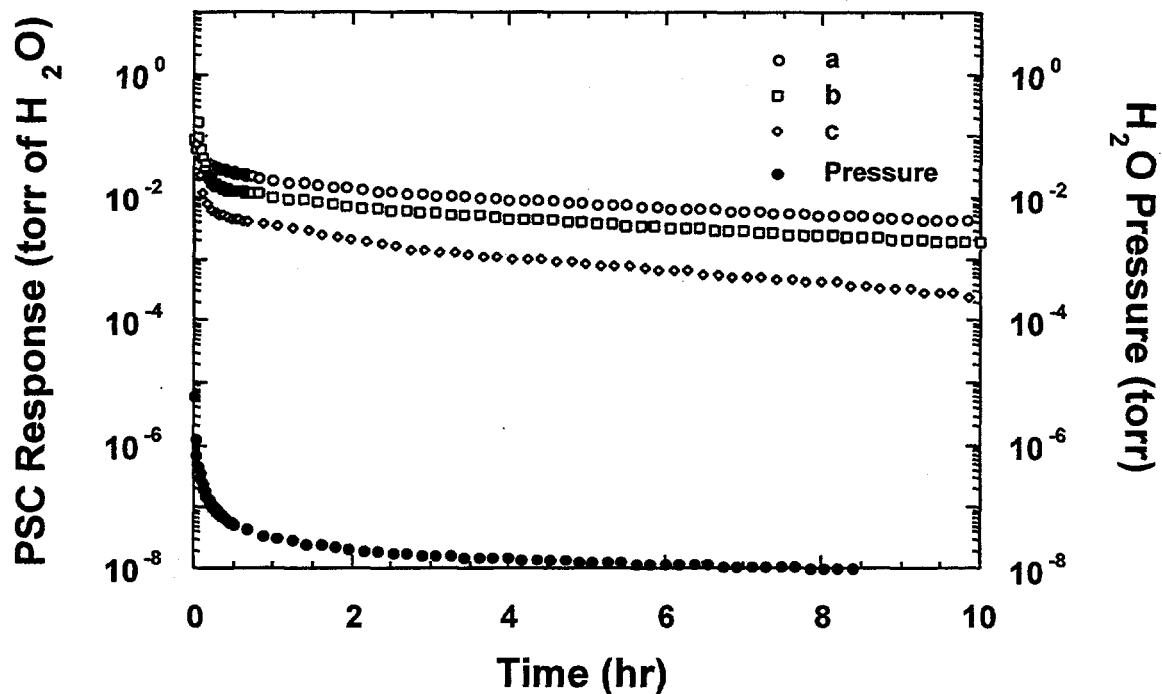


Figure 14: Response Curves for PSC #4B: a) evacuation after 1 torr H₂O exposure, b) evacuation after 1 torr H₂O exposure and a thermal pulse, and c) thermal pulse only.

would be to return the active region of the sensor to a controlled temperature as quickly as possible.

Thermal energy input to the PSC sensor raise concerns about its impact on device sensitivity. Limited thermal pulsing of the sensors appears to increase their sensitivity to moisture. Table 5 displays the sensitivity values for sensor 1A before, after one, and after multiple thermal pulses. The data show that the sensitivity in the 1 to 10 mtorr range increased by ~20% with multiple thermal pulses. Additionally, this enhanced sensitivity is maintained even after atmospheric exposure indicating an irreversible activation of the sensor. The results displayed in Table 5 were

Table 5: Impact of Thermal Pulsing on Sensitivity

Cumulative Thermal Pulses (10W @ 1 sec)	Sensitivity, 1-10 mtorr (pF/torr, pF/ppm _v)	Comments
initial	24.6±0.5, (18.7±0.4)×10 ⁻³	----
1	23±1, (18±1)×10 ⁻³	----
10	28.0±0.5, (21.3±0.4)×10 ⁻³	multiple atmospheric vents prior to heating
12	30.0±0.5, (22.8±0.4)×10 ⁻³	multiple atmospheric vents after heating

collected over a two week period and may reflect effects of sensor aging. However, we generally observe a sensitivity decrease with increased time of vacuum containment in the absence of sensor heating. Consistent with this observed enhancement are measurements made for sensor 5A that showed a sensitivity shift of 31.1 ± 0.5 to 35.1 ± 0.5 pF/torr with a single heat pulse. This result suggests that sensor activation may occur on a more rapid time scale than indicated by the data of Table 5. This observed enhancement in sensitivity falls well within the limits found for a production lot of sensors, indicating that heating has a minor impact on device electrical properties. We have not observed an impact of heating on C_b values other than the drying phenomenon discussed previously.

IV. Conclusions

Our goal in this study was to evaluate the use of the PSC sensor in a vacuum environment. We found that these sensors are capable of detecting moisture levels within the range of 5×10^{-5} to 1 torr (65 ppb_v to 10^3 ppm_v). Calibration studies showed that the response of these sensors is nonlinear with sensitivities of 200 pF/torr (0.15 pF/ppm_v) at low pressures (0.1 to 1 mtorr) to 5 pF/torr (0.004 pF/ppm_v) at high pressures (0.1 to 1 torr). Quantitation is hindered because of aging effects with vacuum containment that yield gradual decreases in both C_b values and sensitivities. We have also shown that the C_b and sensitivity can be affected by contaminant exposure due to the nonselective adsorptive nature of the sensor. Quantitation is dependent on both stable C_b and sensitivity values.

Sensor response time appears to be the major impediment to using these sensors in their current configuration as transient environment monitors. We found that the time required to fully dry the sensor after vacuum installation is on the order of 70 hours. Atmospheric venting of the sensor, as in a load lock application, also requires drying times on the order of 70 hours. Simulated vent tests using lower moisture exposures with pressures in the 0.1 to 1 torr range show similar drying times. Total drying is essential if it is desired to take advantage of the 65 ppb_v LLD of the sensor. Incomplete drying also increases the probable error of a measurement. We estimate that this error can be as large as 50 mtorr at 100 seconds and 6 mtorr at hours after elevated pressure exposure. The slow drying of these sensors is a result of their porous nature and the adsorption process itself. We have demonstrated that the sensors exhibit two discrete regimes of adsorption characterized by significantly varying degrees of reversibility. The lesson learned is that measurements taken at the sensors' LLD will be intrinsically slow. Higher pressure response time characteristics are dictated by conductance limited transport through the porous dielectric structure. Thermal heating of the sensor appears to be one method of decreasing sensor drying times. The concept would be to alter the adsorption energetics and keep H₂O in the vapor phase for a longer period of time at higher velocities. All of these parameters should yield an increase in overall transport rate. We have shown that sensor heating does produce decreases in drying times. We also found that heating can produce a two fold decrease in probable error in measured moisture levels within the first minute of evacuation after 1 torr exposures. Whether this increase in response time is significant will depend upon the applications environment. A second option for increasing response times would be to decrease the thickness of the dielectric layer. A shorter pore length would increase the net conductance from the porous dielectric.

The PSC sensor, in its current configuration, appears to have several restricted application regimes. Sensor response times on the order of 10 seconds would allow its use for transient

moisture detection in the 0.1 torr to atmospheric moisture level regime. Applications that might fall into this category include preventative maintenance cycle monitoring and load lock operations where large outgassing rates occur. Trend analysis of the capacitance decay could be conducted using reference data to minimize measurement error. A second application regime would involve using the sensor in a static environment where response time is not an issue. The sensor could be used to track either gradual moisture changes or to search for anomalous, large scale moisture events. Attention might have to be given to thermal drift in the C_p value to allow for gradual change measurements.

References

1. K. B. Pfeifer, M. J. Kelly, T. R. Guilinger, D. W. Peterson, J. N. Sweet, and M. R. Tuck, "Development of Solid State Moisture Sensors for Semiconductor Fabrication Applications", Proceedings of the Microcontamination 94 Conference, San Jose, CA, October 4-6, 1994.
2. T. R. Guilinger, M. J. Kelly, V. E. Granstaff, D. W. Petersen, J. N. Sweet, and M. R. Tuck, "Vapor Sensors Formed by Chemical Derivatization of Porous Silicon", Proceedings of a Symposium on Electrochemical Microfabrication, 180th Meeting of the Electrochemical Society, Phoenix, AZ, Oct. 13-18, 1991.
3. M. J. Kelly, T. R. Guilinger, D. W. Peterson, M. R. Tuck, and J. N. Sweet, "Oxidized Porous Silicon Moisture Sensors for Evaluation of Microelectronic Packaging", Materials Research Society Proceedings, 1991.
4. J. N. Sweet, D. W. Peterson, M. R. Tuck, M. J. Kelly, and T. R. Guilinger, "Evaluation of Chip Passivation and Coatings Using Special Purpose Assembly Test Chips and Porous Silicon Moisture Detectors", Proceedings of the 41st Electronic Components and Technology Conference, Atlanta, GA, May 13-15, 1991.
5. P.R. Bevington, "Data Reduction and Error Analysis for the Physical Sciences", McGraw-Hill, New York, 1969, p. 92-117.